

**Supporting Information**

**Highly Sensitive and Low-Power Consumption**

**Metalloporphyrin-Based Junctions for CO<sub>x</sub>**

**Detection with Excellent Recovery**

Azar Ostovan,<sup>\*,†</sup> Nick Papior,<sup>‡</sup> and S. Shahab Naghavi<sup>\*,†</sup>

*†Department of Physical and Computational Chemistry, Shahid Beheshti University,  
1983969411 Tehran, Iran*

*‡DTU Computing Center, Department of Applied Mathematics and Computer Science,  
Technical University of Denmark, DK-2800 Kongens Lyngby, Denmark*

E-mail: a\_ostovan@sbu.ac.ir; s\_naghavi@sbu.ac.ir

Table S1: Comparison between the obtained current results at bias=+0.4 V for different ZnPor-based junctions. The structure of the simulated junctions are presented in Figure S3 of SI.

Device	Current ( $\mu A$ )
Au-S-ZnP-S-Au	0.49
Au-S-ZndpP-S-Au	0.47
Au-S-ZntpP-S-Au	0.38
Experiment	0.60

Table S2: Calculated relative adsorption energy ( $E_{ads}$ , eV) of various configurations of CO binding over studied *MPors*. The considered configurations are shown in Figure S2.

Device	$E_A$	$E_B$	$E_T$
Sc	$11 \times 10^{-4}$	$8 \times 10^{-4}$	0.00
Ti	0.78	0.00	0.78
V	1.28	0.00	1.22
Cr	1.69	0.00	1.69
Mn	2.05	0.00	2.05
Fe	0.02	2.29	0.00
Co	$8 \times 10^{-3}$	0.09	0.00
Ni	0.003	0.00	0.003
Cu	0.005	0.01	0.00
Zn	0.002	0.05	0.00

Table S3: Calculated adsorption energy ( $E_{ads}$ , eV), bond length ( $d$ , Å), and difference in Hirshfeld charge (CT) of central ion-magnet after CO adsorption.

Device	$E_{ads}$	$d$	CT
Sc	-1.27	2.33	-0.32
Ti	-1.88	2.07	-0.86
V	-1.49	2.00	-0.39
Cr	-0.11	2.63	-0.07
Mn	-0.40	2.39	-0.12
Fe	-1.23	1.74	-0.41
Co	-1.01	1.86	-0.19
Ni	-0.08	2.20	-0.02
Cu	-0.20	1.85	-0.11
Zn	-0.38	1.37	-0.13

Table S4: Calculated recovery time ( $\tau$ , s) of CO gas from *M*Por based devices.

Device	$\tau$
Sc	$2.00 \times 10^{+9}$
Ti	$1.1 \times 10^{+21}$
V	$11.46 \times 10^{+13}$
Cr	$16.67 \times 10^{-12}$
Mn	$1.2 \times 10^{-6}$
Fe	$6.45 \times 10^7$
Co	$13.50 \times 10^1$
Ni	$4.25 \times 10^{-12}$
Cu	$5.53 \times 10^{-9}$
Zn	$0.6 \times 10^{-6}$

Table S5: Calculated relative stabilization energy (eV) of various configurations of CO<sub>2</sub> adsorption on studied MPors. The considered configurations are shown in Figure S12.

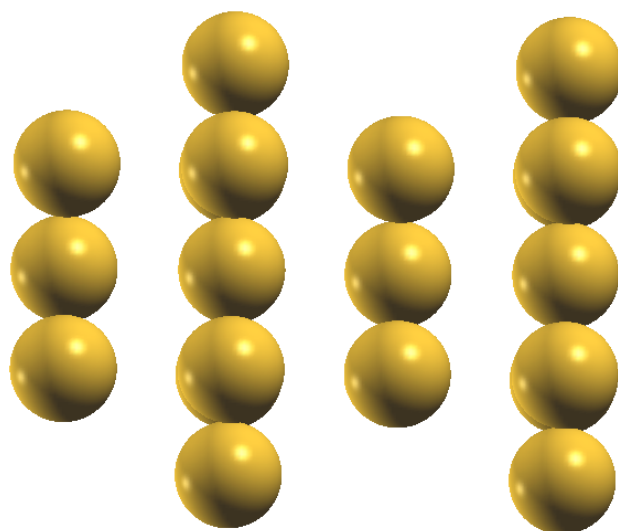
Device	$E_{CB}$	$E_{OB}$	$E_T$
Sc	0.04	0.02	0.00
Ti	0.04	0.00	0.78
V	1.28	0.00	0.89
Cr	1.69	0.00	1.69
Mn	2.05	0.00	2.05
Fe	0.00	2.29	0.10
Co	$8 \times 10^{-3}$	0.00	0.09
Ni	0.003	0.00	0.003
Cu	0.005	0.01	0.00
Zn	0.002	0.00	0.05

Table S6: Calculated adsorption energy ( $E_{ads}$ , eV), bond length ( $d$ , Å), and difference in Hirshfeld charge ( $q$ ) of central ion-magnet after CO<sub>2</sub> adsorption.

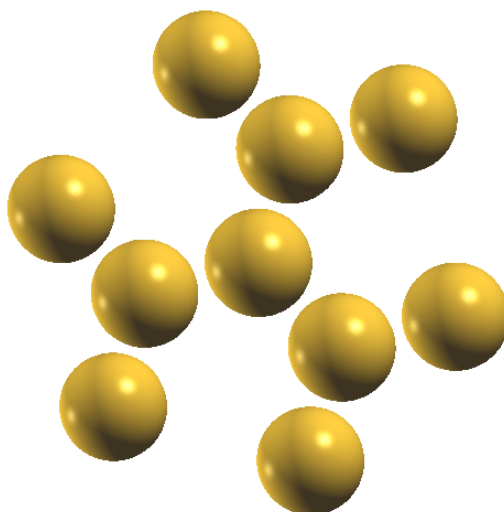
Device	$E_{ads}$	$d$	$q$
Sc	-0.51	2.10	0.098
Ti	-0.72	1.94	0.420
V	-0.39	2.71	0.088
Cr	-0.08	3.03	0.014
Mn	-0.38	2.00	0.072
Fe	-0.43	2.08	0.096
Co	-0.68	2.00	0.114
Ni	-0.06	3.31	0.012
Cu	-0.11	3.00	0.014
Zn	-0.35	2.47	0.034

Table S7: Calculated recovery time ( $\tau$ , s) of CO<sub>2</sub> gas from MPor based devices.

Device	$\tau$
Sc	$1 \times 10^{-8}$
Ti	13
V	$0.52 \times 10^{-9}$
Cr	$22 \times 10^{-16}$
Mn	$0.17 \times 10^{-8}$
Fe	$0.29 \times 10^{-9}$
Co	$0.05 \times 10^{-3}$
Ni	$10 \times 10^{-16}$
Cu	$70 \times 10^{-16}$
Zn	$0.75 \times 10^{-10}$



(a) side view of Au electrode



(b) top view of Au electrode

Figure S1: (a) Side and (b) Top view Au electrodes used for setting up of the molecular sensors in this study.

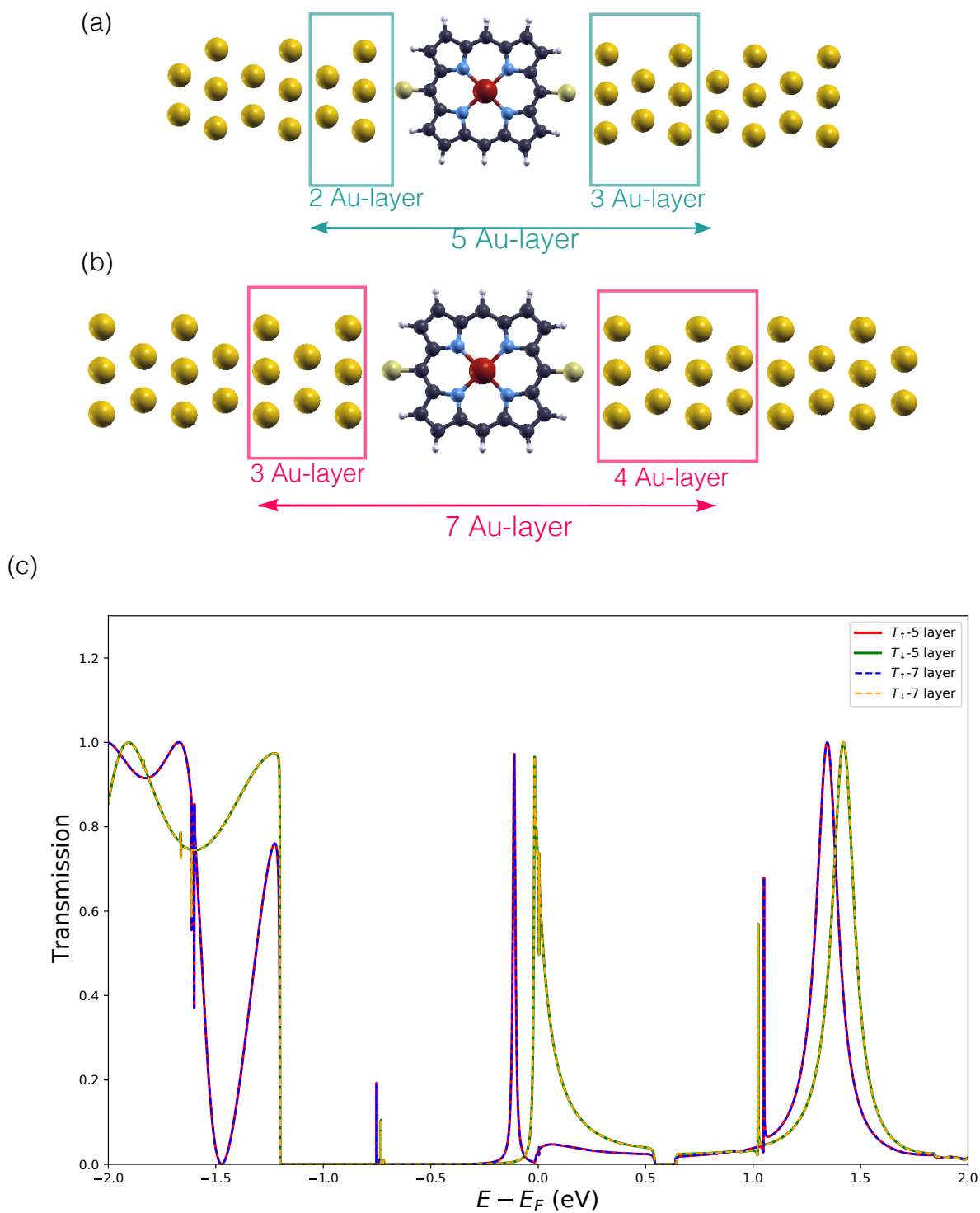


Figure S2: The structure of Au–S–FeP–S–Au system with (a) 5 Au layer and (b) 7 Au layer in extended scattering region to screen the suitable number of Au layer should be included in extended central region to avoid lateral molecule interaction and direct electrode-electrode transmission. (c) The spin-polarized transmission coefficients of junctions are shown in Figure (a) and (b). The transmission coefficients for major and minor-spins do not change by extending the central region from 5 to 7 Au layers ( sum of left and right layers).

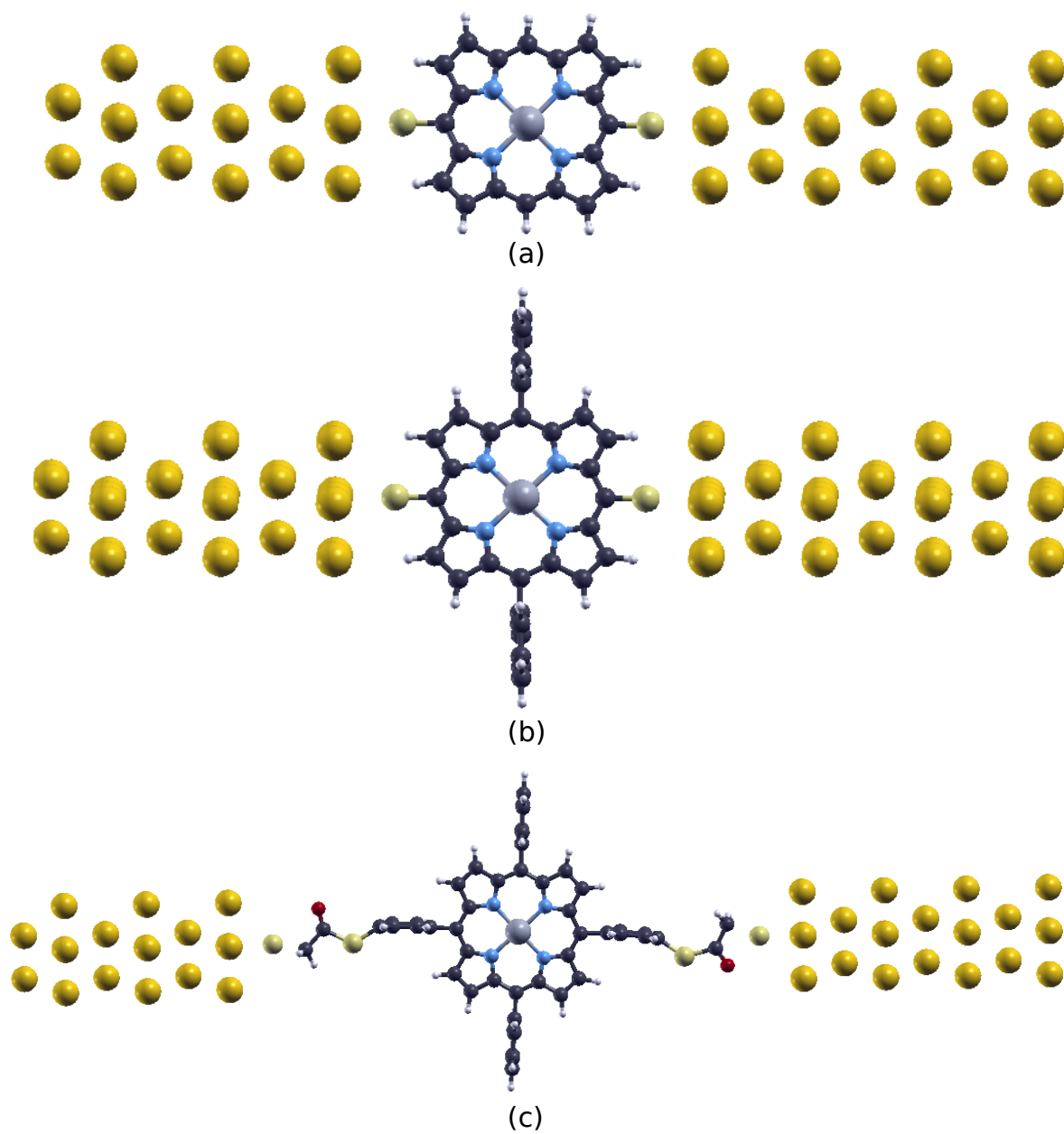


Figure S3: The structure of (a) Au-S-ZnP-S-Au, (b) Au-S-ZndpP-S-Au, and (c) Au-S-ZntpP-S-Au junctions are used to compare the conductance properties of MPors with different side groups.

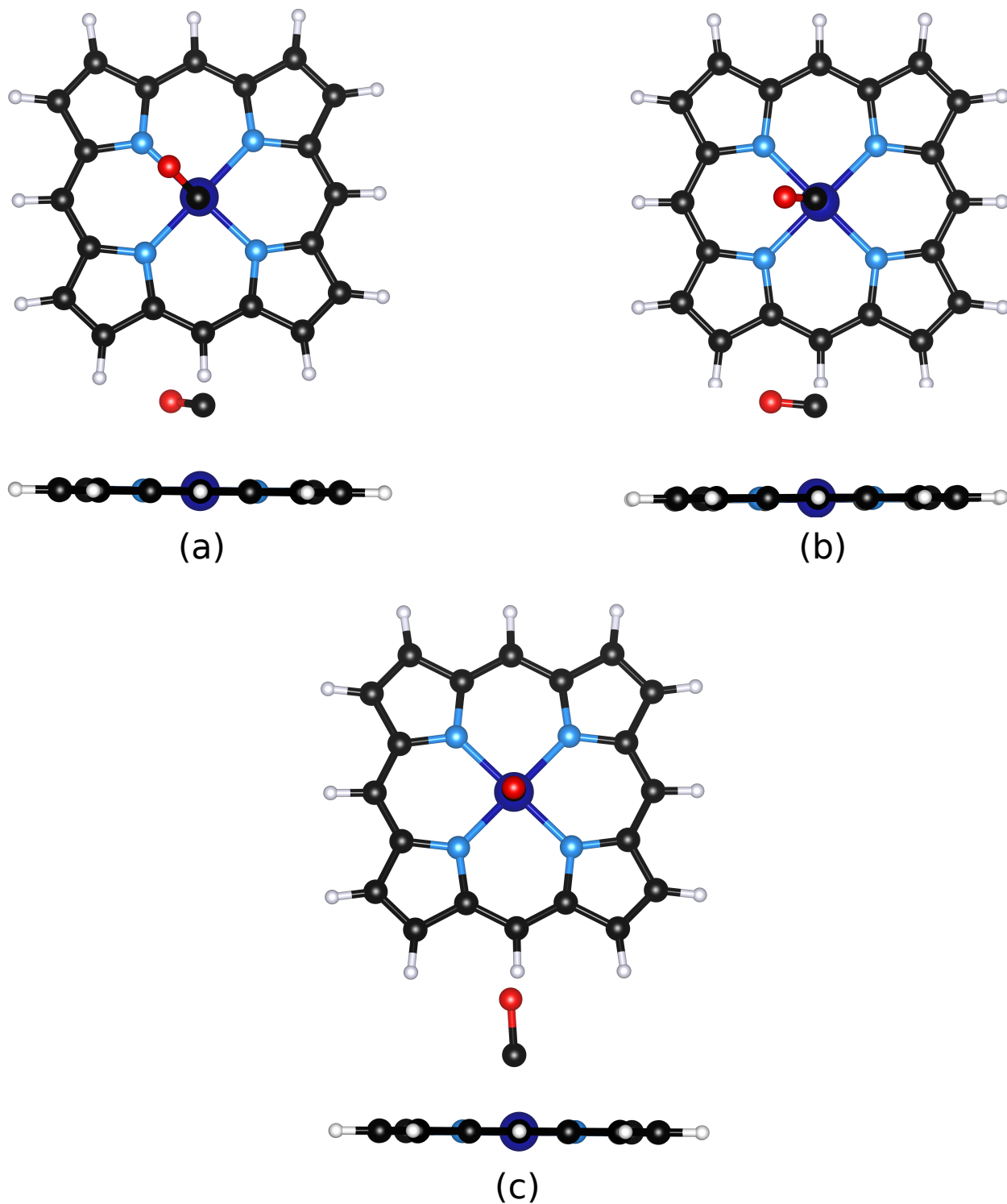


Figure S4: Different CO adsorption configurations: (a) The CO gas is located along the two pyrrole rings: A-configuration. (b) The CO gas is placed between the two pyrrole rings: B-configuration. (c) The CO gas is placed on the top of the central ion-magnet: C-configuration. In all three configurations the CO gas is coordinated through the carbon atom.

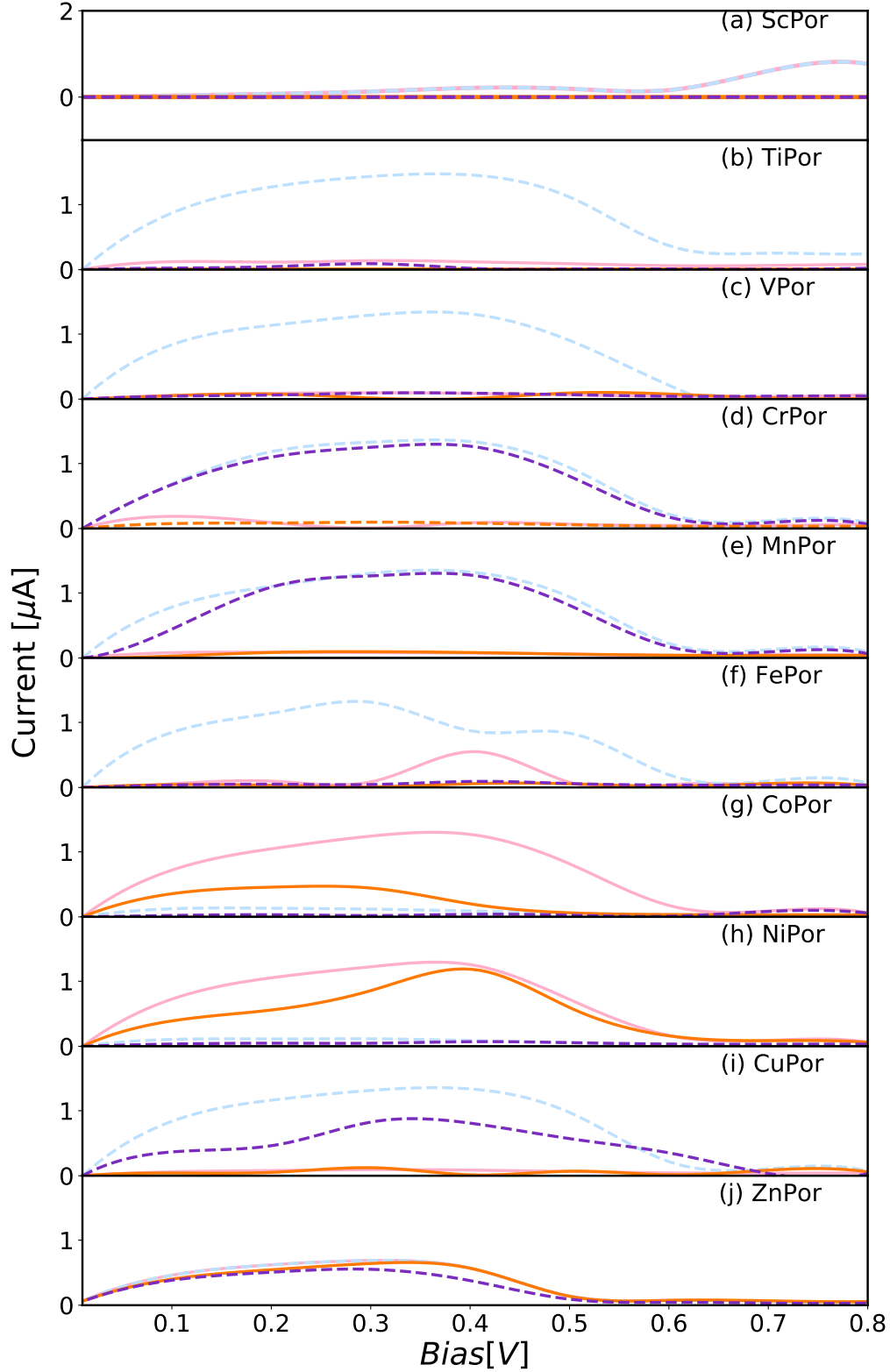


Figure S5: Calculated spin-resolved  $I - V$  curves of the pristine Au-MPor-Au and Au-CO@MPor-Au devices. The light pink and light blue colors represent the obtained  $I_{\uparrow}$  and  $I_{\downarrow}$  for Au-MPor-Au devices. The  $I_{\uparrow}$  and  $I_{\downarrow}$  of CO adsorbed devices are shown by orange and purple. The dashed curves represent the  $I_{\downarrow}$  of devices before and after CO adsorption. For simplicity, each plot is labeled by the device centered molecule

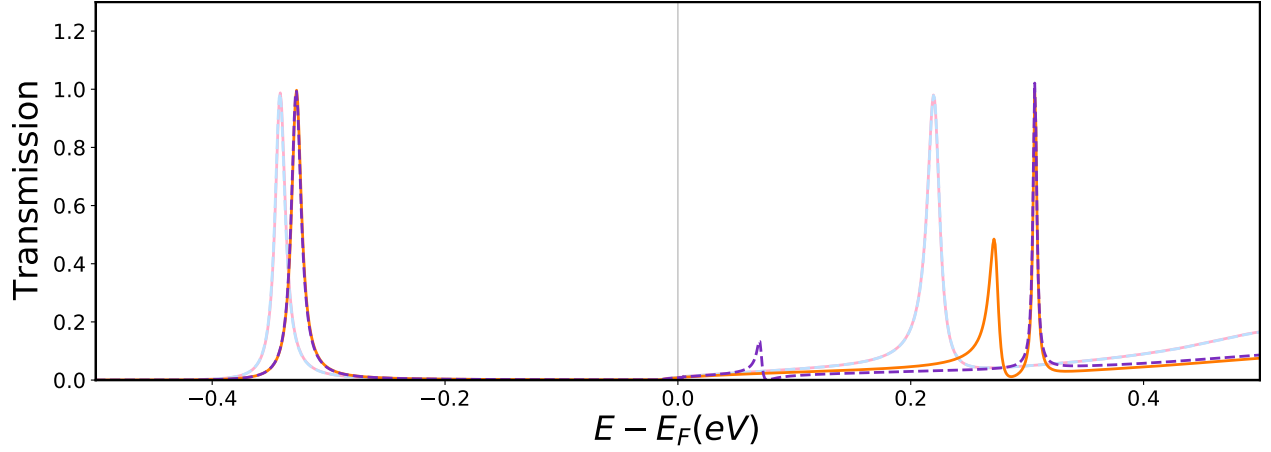


Figure S6: Spin-resolved transmission functions of Au-ScPor-Au and Au-CO@ScPor-Au at 0.0 bias voltages. The light pink and light blue colors represent the obtained  $T_{\uparrow}$  and  $T_{\downarrow}$  for Au-MPor-Au devices. The  $T_{\uparrow}$  and  $T_{\downarrow}$  of CO adsorbed devices are shown by orange and purple. The dashed curves represent the  $T_{\downarrow}$  of devices before and after CO adsorption.

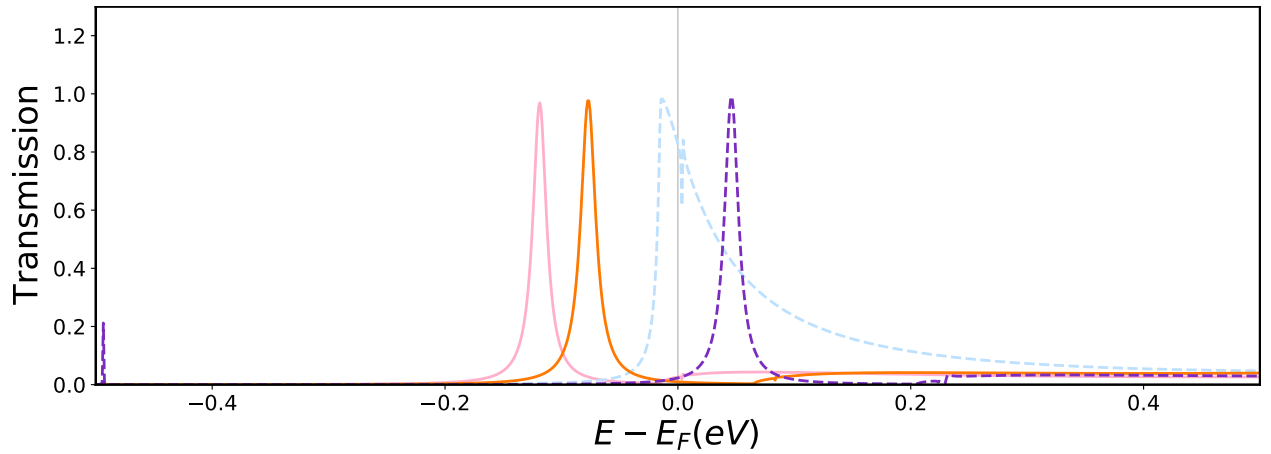


Figure S7: Spin-resolved transmission functions of Au-VPor-Au and Au-CO@VPor-Au at 0.0 bias voltages. The light pink and light blue colors represent the obtained  $T_{\uparrow}$  and  $T_{\downarrow}$  for Au-MPor-Au devices. The  $T_{\uparrow}$  and  $T_{\downarrow}$  of CO adsorbed devices are shown by orange and purple. The dashed curves represent the  $T_{\downarrow}$  of devices before and after CO adsorption.

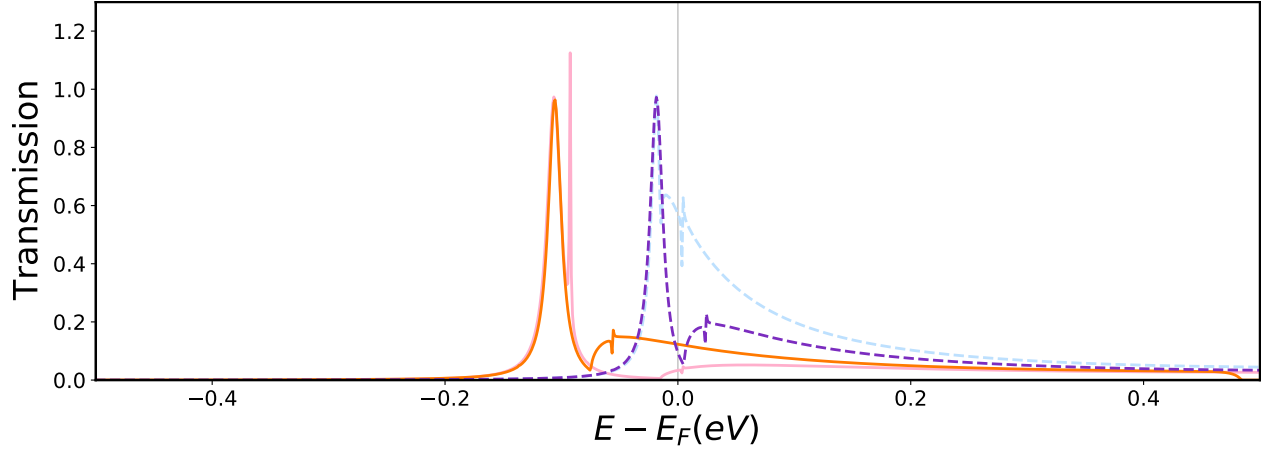


Figure S8: Spin-resolved transmission functions of Au-MnPor-Au and Au-CO@MnPor-Au at 0.0 bias voltages. The light pink and light blue colors represent the obtained  $T_{\uparrow}$  and  $T_{\downarrow}$  for Au-MnPor-Au devices. The  $T_{\uparrow}$  and  $T_{\downarrow}$  of CO adsorbed devices are shown by orange and purple. The dashed curves represent the  $T_{\downarrow}$  of devices before and after CO adsorption.

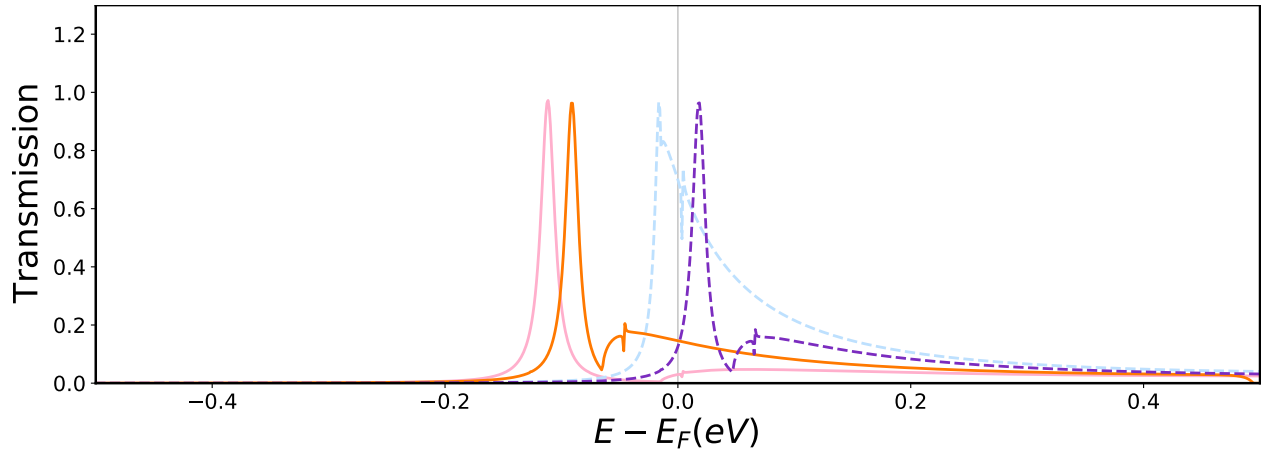


Figure S9: Spin-resolved transmission functions of Au-FePor-Au and Au-CO@FePor-Au at 0.0 bias voltages. The light pink and light blue colors represent the obtained  $T_{\uparrow}$  and  $T_{\downarrow}$  for Au-FePor-Au devices. The  $T_{\uparrow}$  and  $T_{\downarrow}$  of CO adsorbed devices are shown by orange and purple. The dashed curves represent the  $T_{\downarrow}$  of devices before and after CO adsorption.

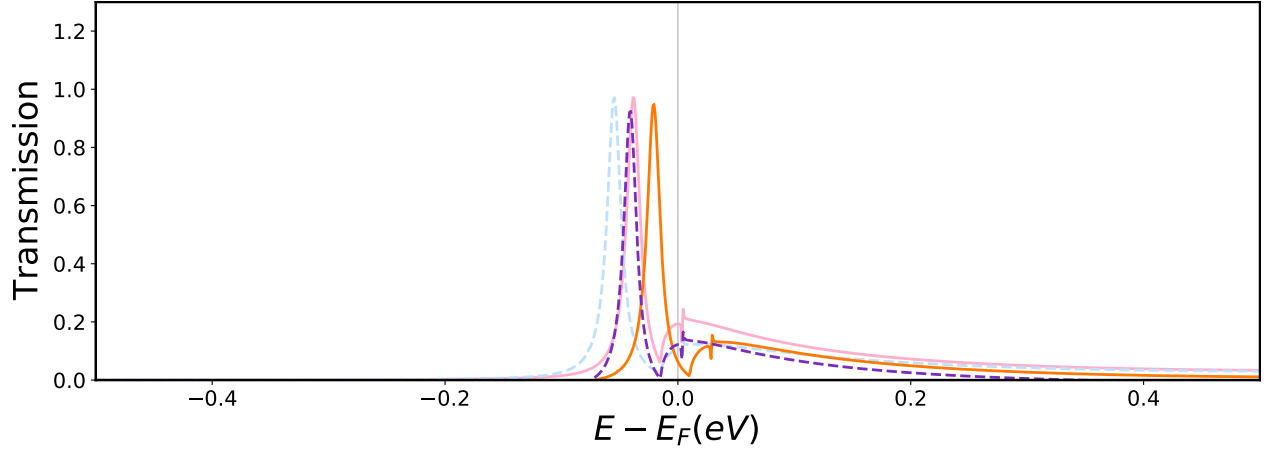


Figure S10: Spin-resolved transmission functions of Au-CoPor-Au and Au-CO@CoPor-Au at 0.0 bias voltages. The light pink and light blue colors represent the obtained  $T_{\uparrow}$  and  $T_{\downarrow}$  for Au-MPor-Au devices. The  $T_{\uparrow}$  and  $T_{\downarrow}$  of CO adsorbed devices are shown by orange and purple. The dashed curves represent the  $T_{\downarrow}$  of devices before and after CO adsorption.

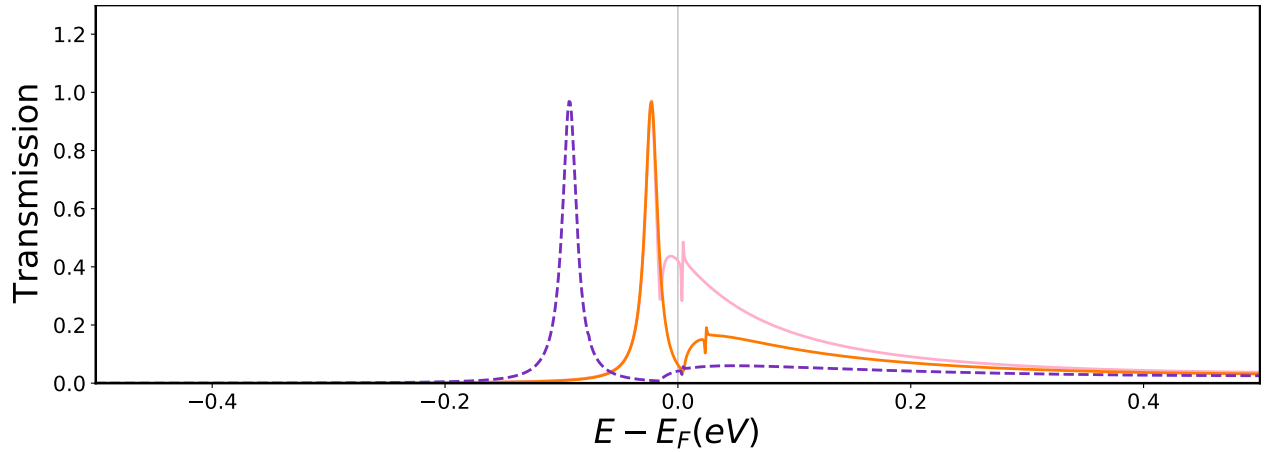


Figure S11: Spin-resolved transmission functions of Au-NiPor-Au and Au-CO@NiPor-Au at 0.0 bias voltages. The light pink and light blue colors represent the obtained  $T_{\uparrow}$  and  $T_{\downarrow}$  for Au-MPor-Au devices. The  $T_{\uparrow}$  and  $T_{\downarrow}$  of CO adsorbed devices are shown by orange and purple. The dashed curves represent the  $T_{\downarrow}$  of devices before and after CO adsorption.

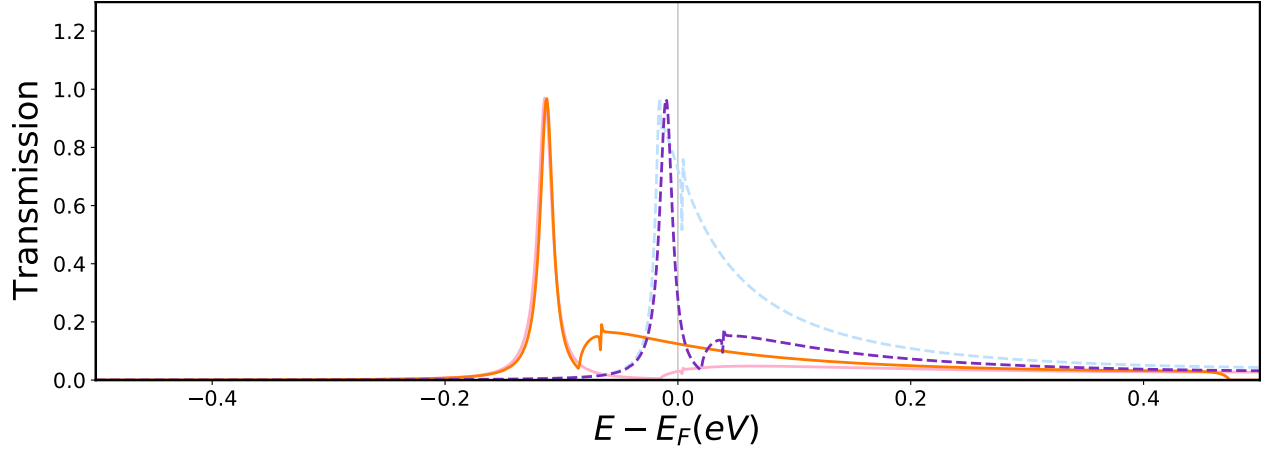


Figure S12: Spin-resolved transmission functions of Au-CuPor-Au and Au-CO@CuPor-Au at 0.0 bias voltages. The light pink and light blue colors represent the obtained  $T_{\uparrow}$  and  $T_{\downarrow}$  for Au-MPor-Au devices. The  $T_{\uparrow}$  and  $T_{\downarrow}$  of CO adsorbed devices are shown by orange and purple. The dashed curves represent the  $T_{\downarrow}$  of devices before and after CO adsorption.

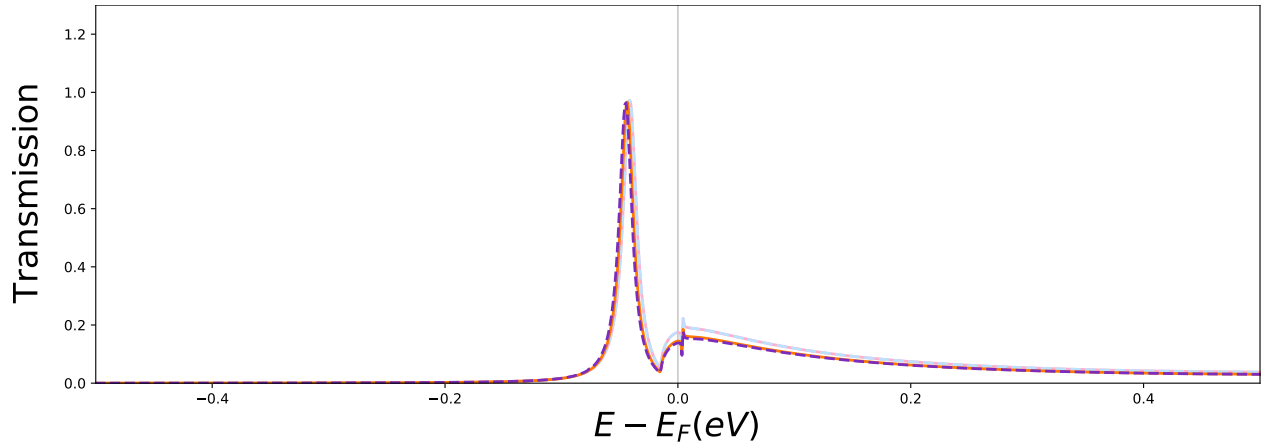


Figure S13: Spin-resolved transmission functions of Au-ZnPor-Au and Au-CO@ZnPor-Au at 0.0 bias voltages. The light pink and light blue colors represent the obtained  $T_{\uparrow}$  and  $T_{\downarrow}$  for Au-MPor-Au devices. The  $T_{\uparrow}$  and  $T_{\downarrow}$  of CO adsorbed devices are shown by orange and purple. The dashed curves represent the  $T_{\downarrow}$  of devices before and after CO adsorption.

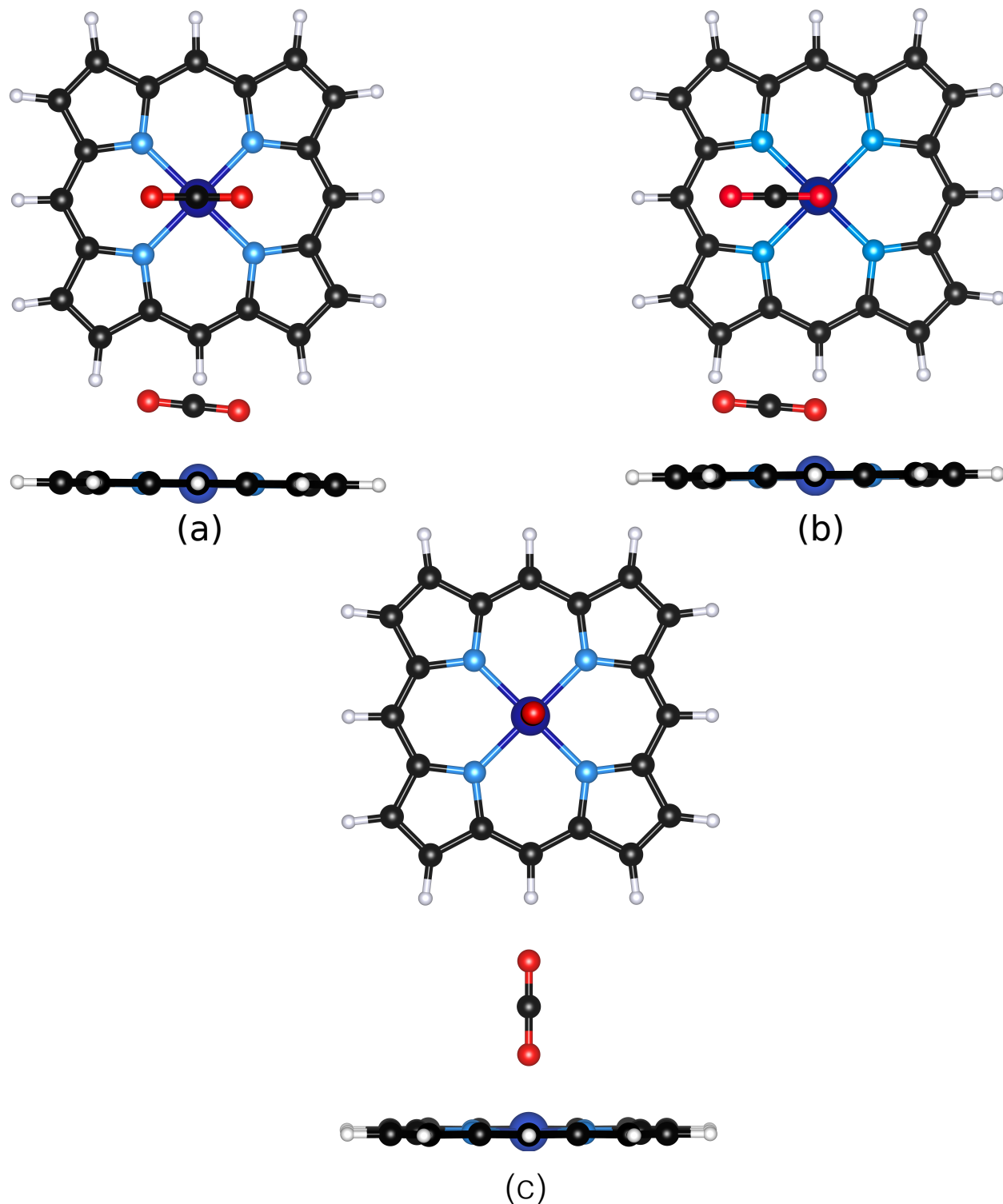


Figure S14: Different CO<sub>2</sub> adsorption configuration (a) The CO<sub>2</sub> gas is located along the two pyrrole rings and is coordinated through the carbon atom: A-configuration. (b) The CO<sub>2</sub> gas is placed between the two pyrrole rings and is coordinated through the carbon atom: B-configuration. (c) The CO<sub>2</sub> gas is placed on the top of the central ion-magnet T-configuration.

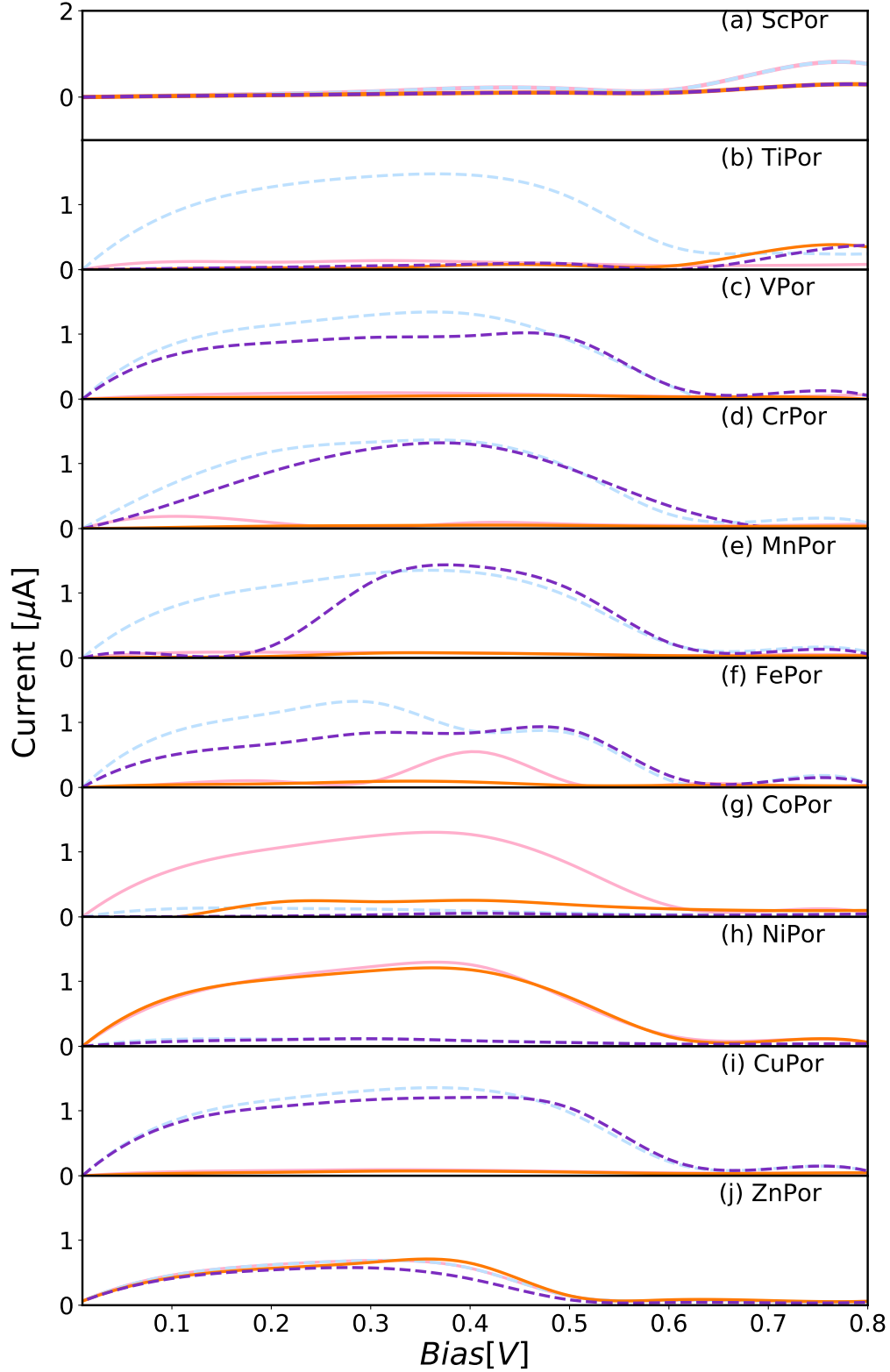


Figure S15: Calculated spin-resolved  $I - V$  curves of the pristine Au-MPor-Au and Au-CO<sub>2</sub>@MPor-Au devices. The light pink and light blue colors represent the obtained  $I_{\uparrow}$  and  $I_{\downarrow}$  for Au-MPor-Au devices. The  $I_{\uparrow}$  and  $I_{\downarrow}$  of CO<sub>2</sub> adsorbed devices are shown by orange and purple. The dashed curves represent the  $I_{\downarrow}$  of devices before and after CO<sub>2</sub> adsorption. For simplicity, each plot is labeled by the device centered molecule

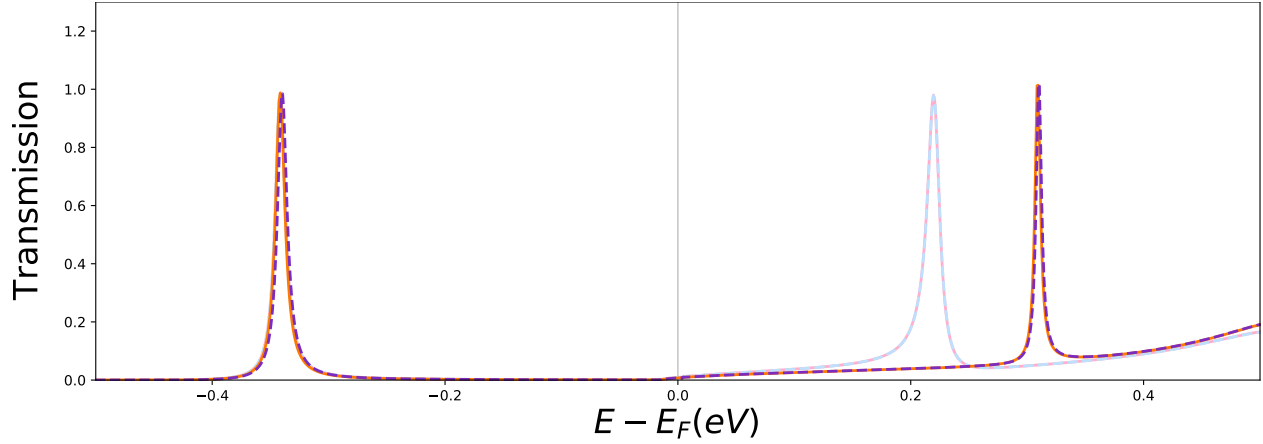


Figure S16: Spin-resolved transmission functions of Au-ScPor-Au and Au-CO@ScPor-Au at 0.0 bias voltages. The light pink and light blue colors represent the obtained  $T_{\uparrow}$  and  $T_{\downarrow}$  for Au-MPor-Au devices. The  $T_{\uparrow}$  and  $T_{\downarrow}$  of CO<sub>2</sub> adsorbed devices are shown by orange and purple. The dashed curves represent the  $T_{\downarrow}$  of devices before and after CO<sub>2</sub> adsorption.

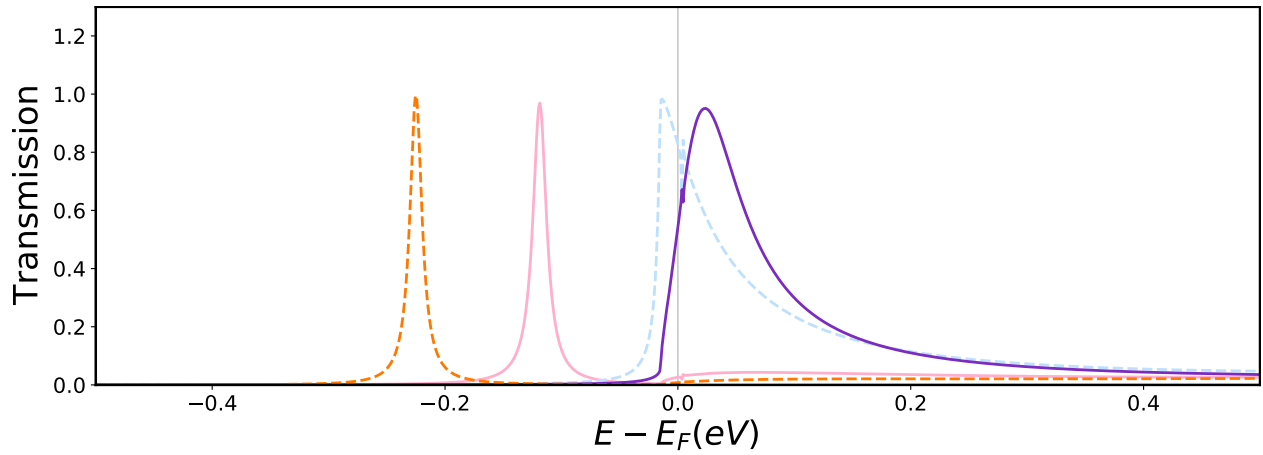


Figure S17: Spin-resolved transmission functions of Au-VPor-Au and Au-CO@VPor-Au at 0.0 bias voltages. The light pink and light blue colors represent the obtained  $T_{\uparrow}$  and  $T_{\downarrow}$  for Au-MPor-Au devices. The  $T_{\uparrow}$  and  $T_{\downarrow}$  of CO<sub>2</sub> adsorbed devices are shown by orange and purple. The dashed curves represent the  $T_{\downarrow}$  of devices before and after CO<sub>2</sub> adsorption.

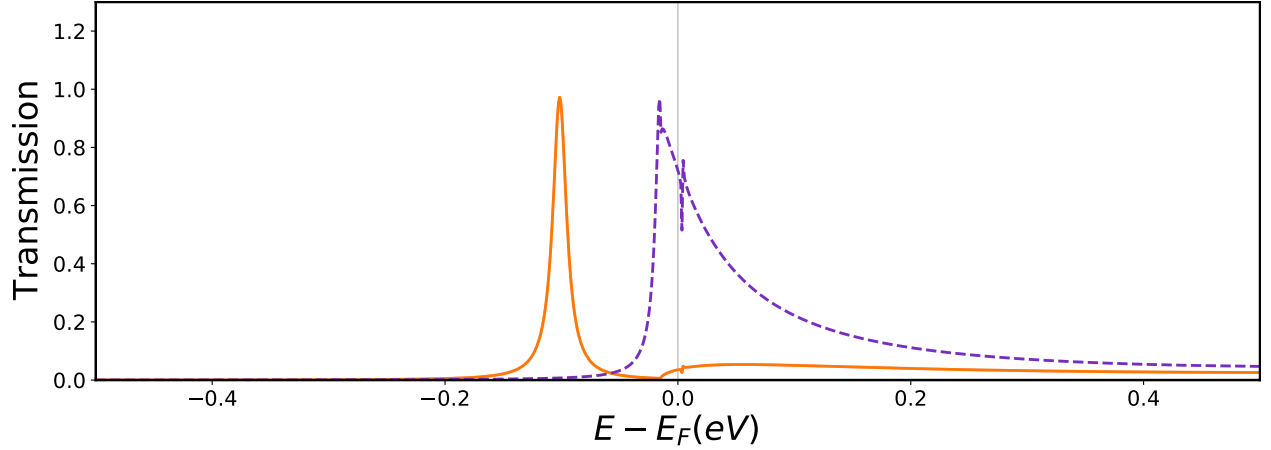


Figure S18: Spin-resolved transmission functions of Au-CrPor-Au and Au-CO@CrPor-Au at 0.0 bias voltages. The light pink and light blue colors represent the obtained  $T_{\uparrow}$  and  $T_{\downarrow}$  for Au-MPor-Au devices. The  $T_{\uparrow}$  and  $T_{\downarrow}$  of CO<sub>2</sub> adsorbed devices are shown by orange and purple. The dashed curves represent the  $T_{\downarrow}$  of devices before and after CO<sub>2</sub> adsorption.

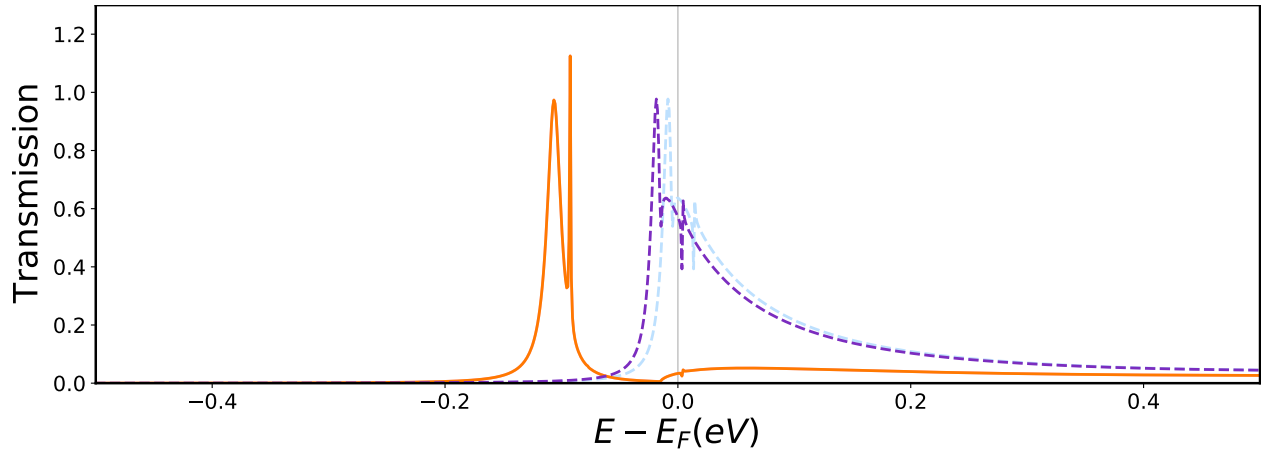


Figure S19: Spin-resolved transmission functions of Au-MnPor-Au and Au-CO@MnPor-Au at 0.0 bias voltages. The light pink and light blue colors represent the obtained  $T_{\uparrow}$  and  $T_{\downarrow}$  for Au-MPor-Au devices. The  $T_{\uparrow}$  and  $T_{\downarrow}$  of CO<sub>2</sub> adsorbed devices are shown by orange and purple. The dashed curves represent the  $T_{\downarrow}$  of devices before and after CO<sub>2</sub> adsorption.

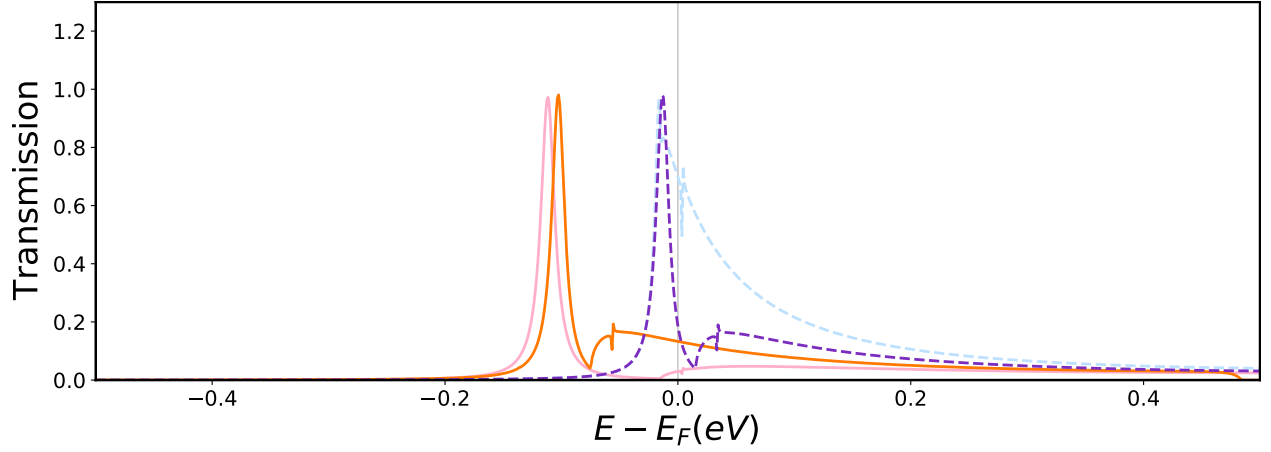


Figure S20: Spin-resolved transmission functions of Au-FePor-Au and Au-CO@FePor-Au at 0.0 bias voltages. The light pink and light blue colors represent the obtained  $T_{\uparrow}$  and  $T_{\downarrow}$  for Au-MPor-Au devices. The  $T_{\uparrow}$  and  $T_{\downarrow}$  of CO<sub>2</sub> adsorbed devices are shown by orange and purple. The dashed curves represent the  $T_{\downarrow}$  of devices before and after CO<sub>2</sub> adsorption.

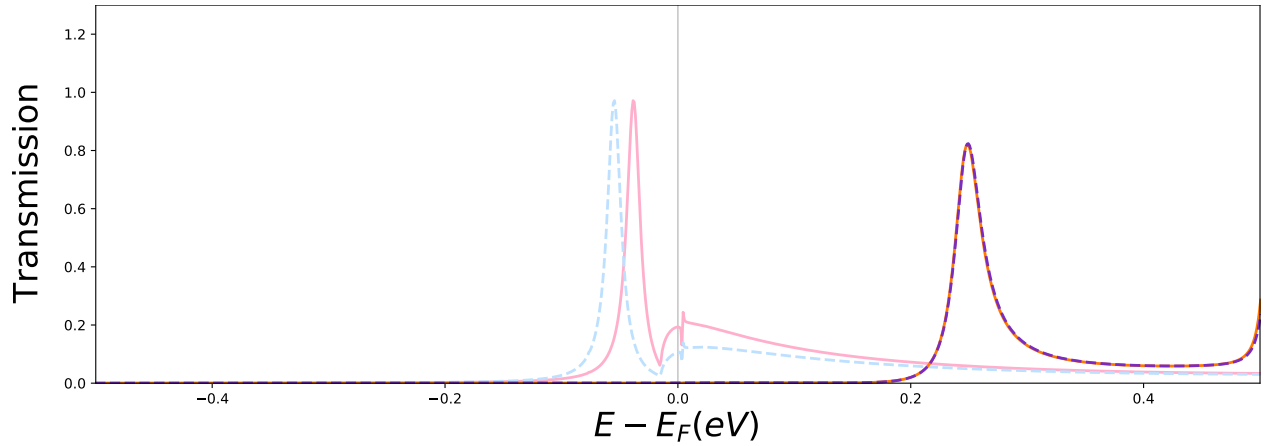


Figure S21: Spin-resolved transmission functions of Au-CoPor-Au and Au-CO@CoPor-Au at 0.0 bias voltages. The light pink and light blue colors represent the obtained  $T_{\uparrow}$  and  $T_{\downarrow}$  for Au-MPor-Au devices. The  $T_{\uparrow}$  and  $T_{\downarrow}$  of CO<sub>2</sub> adsorbed devices are shown by orange and purple. The dashed curves represent the  $T_{\downarrow}$  of devices before and after CO<sub>2</sub> adsorption.

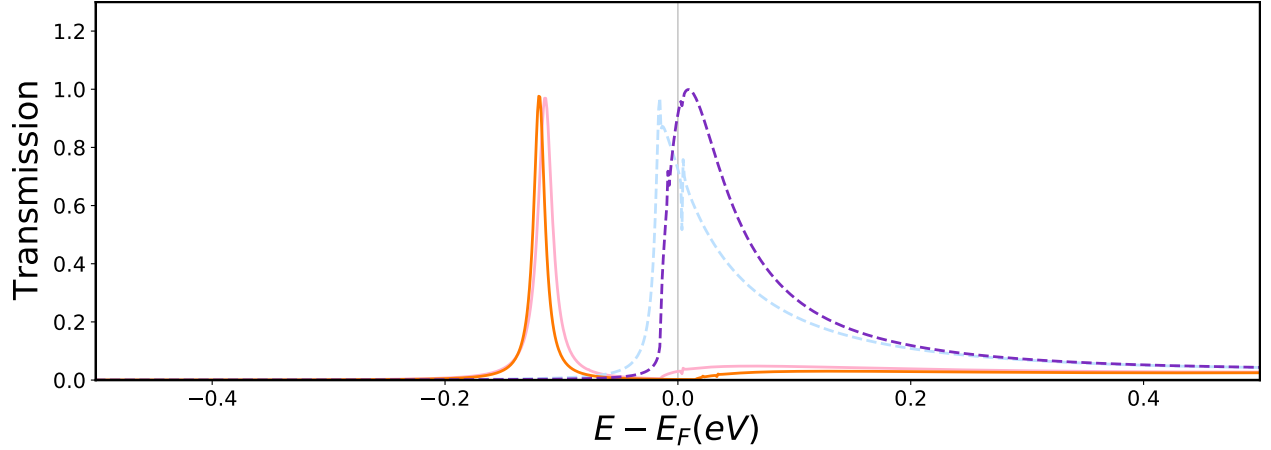


Figure S22: Spin-resolved transmission functions of Au-CuPor-Au and Au-CO@CuPor-Au at 0.0 bias voltages. The light pink and light blue colors represent the obtained  $T_{\uparrow}$  and  $T_{\downarrow}$  for Au-MPor-Au devices. The  $T_{\uparrow}$  and  $T_{\downarrow}$  of CO<sub>2</sub> adsorbed devices are shown by orange and purple. The dashed curves represent the  $T_{\downarrow}$  of devices before and after CO<sub>2</sub> adsorption.

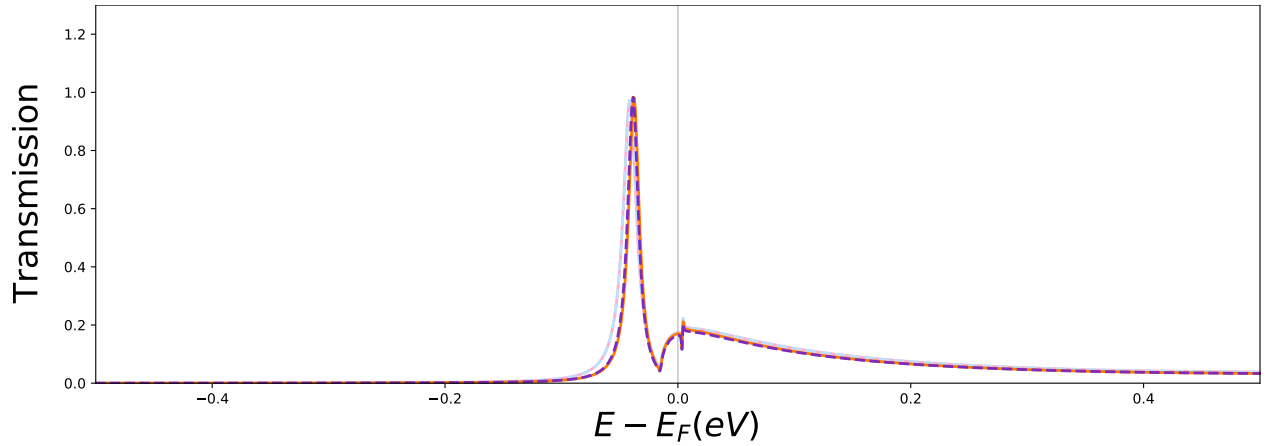


Figure S23: Spin-resolved transmission functions of Au-ZnPor-Au and Au-Zn@CoPor-Au at 0.0 bias voltages. The light pink and light blue colors represent the obtained  $T_{\uparrow}$  and  $T_{\downarrow}$  for Au-MPor-Au devices. The  $T_{\uparrow}$  and  $T_{\downarrow}$  of CO<sub>2</sub> adsorbed devices are shown by orange and purple. The dashed curves represent the  $T_{\downarrow}$  of devices before and after CO<sub>2</sub> adsorption.